Supplementary Information (SI) for Journal of Materials Chemistry A.

Supplementary Information for

Establishing Design Principles for Functional Additives in Antimony Chalcogenide Solar Cells

Matthew Sutton[1], Neil Robertson[2], Tayebeh Ameri[1,3,4*]

[1] Institute for Materials and Processes, School of Engineering, University of Edinburgh, Sanderson Building, Robert Stevenson Road, Edinburgh EH9 3FB, UK.

[2] School of Chemistry, The University of Edinburgh, David Brewster Road, Edinburgh EH9 3FJ, U.K

[3] Chair for Composite Materials, Department of Materials Science, Faculty of Engineering, Christian-Albrechts-Universität zu Kiel, Kaiserstrasse 2, 24143 Kiel, Germany.

[4] Kiel Nano, Surface and Interface Science KiNSIS, Kiel University, Christian-Albrechts-Platz 4, D-24118 Kiel, Germany.

* Corresponding author, Email: tam@tf.uni-kiel.de

Table of Contents

Supplementary Equation 1: Texture Coefficient for Powder X-Ray Diffraction

$$TC_{(hkl)} = I_{(hkl)}/I^0_{(hkl)} \qquad (1)$$

Equation S1 shows texture coefficient (TC), where (hkl) is a specific reflection, $I_{(hkl)}$ is the measured intensity of that reflection in p-XRD, and $I^0_{(hkl)}$ is the standard intensity of that reflection (in this case, ICSD coll. code 30779 - Sb_2S_3)

Supplementary Discussion 1: Justification for the Use of Sb_2S_3/TiO_2 System

Each of the aforementioned studies used CdS as the electron transport layer (ETL). This poses an issue, as CdS suffers from parasitic light absorption[1-3] and arguably more importantly is toxic[2-5], which would restrict its use in commercial products. We therefore chose to investigate a benign system using TiO_2 instead of CdS[1, 3, 4, 6]. $Sb_2(S, Se)_3/TiO_2$ solar cells face issues with consistent deposition on TiO_2, therefore, we chose to use Sb_2S_3 both as a simpler analogue to the Sb_2X_3 system, and to allow for the use of TiO_2. The effective deposition of Sb_2X_3 onto TiO_2 and other stable, benign ETL materials is an area worthy of further research.

Supplementary Discussion 2: Additional Effects of HCl in Additive Screening Process

Among the 10 red powder forming additives, HCl was an outlier. This was likely related to the effect we observed during the screening process whereby after mixing HCl with the precursors, a persistent, yellow precipitate was seen. Other additives had produced some orange-yellow powders, but these all very quickly turned to red colours. This persistent yellow powder, therefore, likely indicated the precipitation of a different chemical. The commonly known reaction $Na_2S_2O_3(s) + 2HCl(aq) \rightarrow 2NaCl(aq) + H_2O(l) + SO_2(g) + S(s)$ produces NaCl and solid sulfur, which would appear as a yellow precipitate. This reaction removed useable (dissolved) sulfur from the solution, so would have negatively impacted the ratio of Sb : S in the final film, and thus negatively impacted performance. This reaction occurs due to the presence of H^+ ions, and so we wondered why it did not occur for the other acidic additives. We concluded that it probably does occur, but very weakly. It is a 2-ion reaction, requiring two H^+ ions for the reaction to go to completion. Therefore, the strong acid HCl would be more able to perform this reaction, as the pH is ~1 lower than the other acidic additives due to complete dissociation, translating to a ~10x increase in $[H^+]$. On the other hand, the weak carboxylic acids of the other additives would restrict availability of H^+ due to the reassociation of H^+ ions to the carboxylic acid groups, thereby not providing enough H^+ for the reaction to occur at a noticeable level.

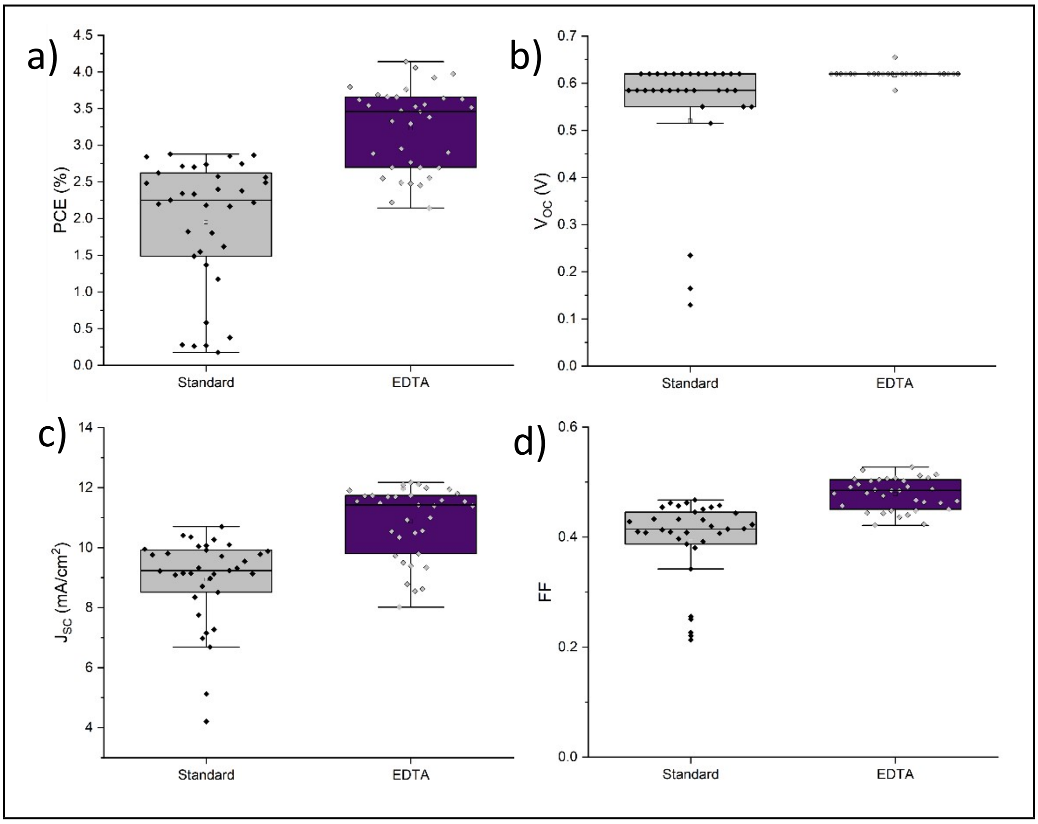

Supplementary Figure 1: Statistics for cell performance characteristics a) PCE, b) V_{OC}, c) J_{SC} and d) FF of standard and EDTA Sb_2S_3 solar cells. 6 cells were tested with 6 pixels per cell for a total of 36 pixels for each standard and EDTA. One pixel from each was fully shunted and so was excluded from the final data as it did not yield any photovoltaic performance.

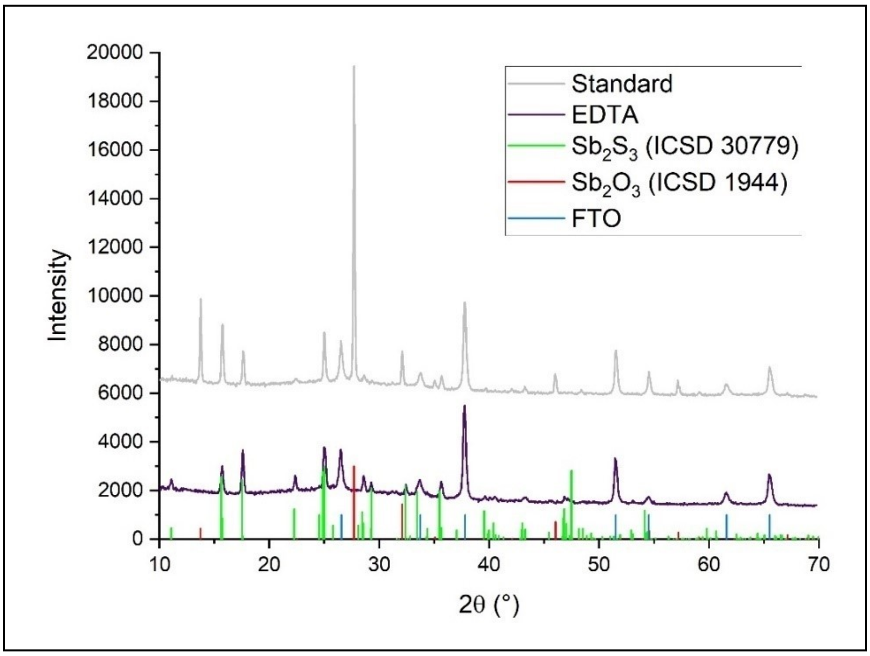

Supplementary Figure 2: Powder XRD of Sb_2S_3 films with and without EDTA, with ICSD standards for Sb_2S_3 (ICSD collection code 30779) and Sb_2O_3 (ICSD collection code 1944), and internally measured standard for FTO.

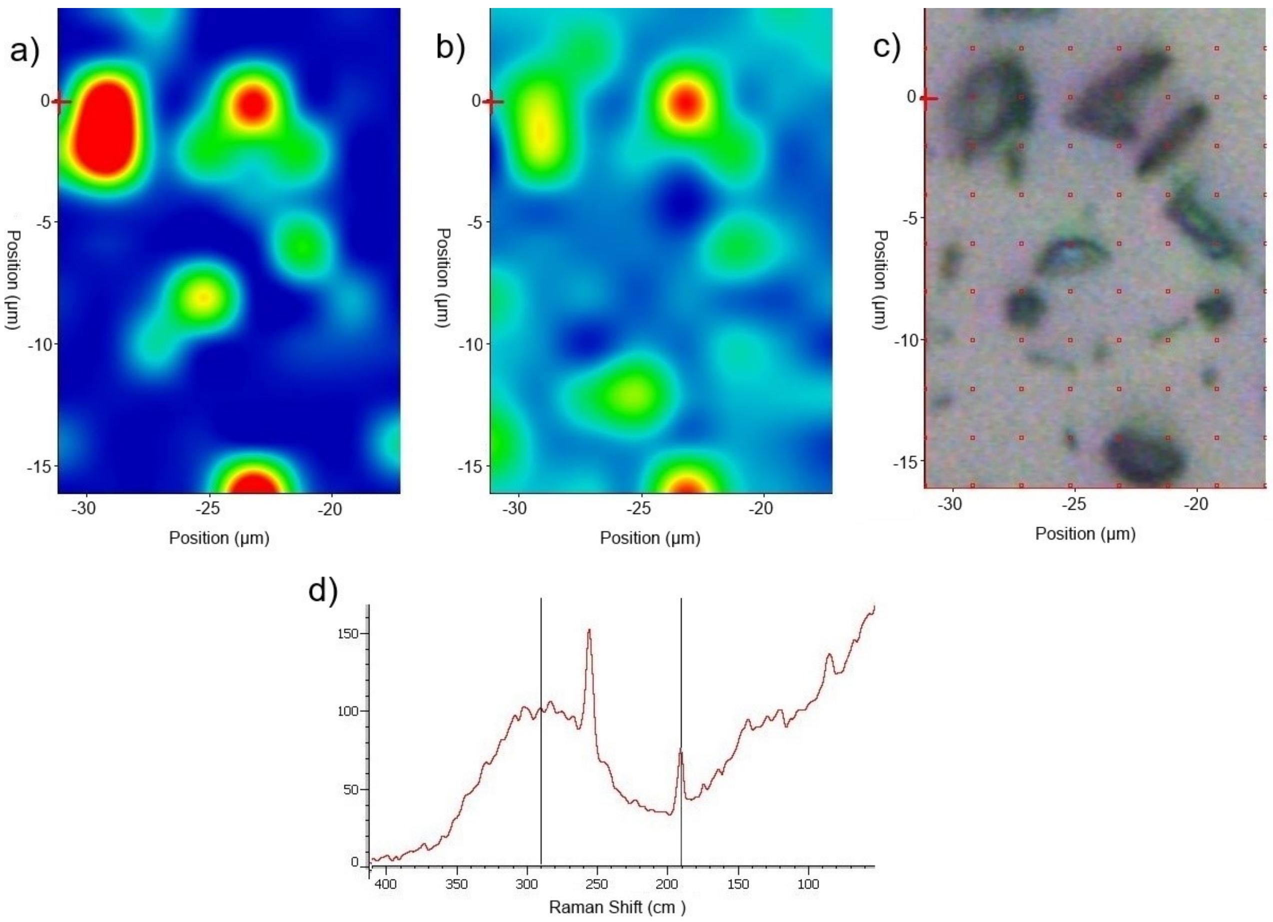

Supplementary Figure 3: Raman intensity maps of a standard (no additive) film for Raman shifts of a) 190 cm^{-1} (corresponding to Sb_2O_3) and b) 290 cm^{-1} (corresponding to Sb_2S_3), optical microscope image c) of the same standard film, showing black crystals which correspond to areas of Sb_2O_3 and the Raman spectrum of an area on the film containing both 190 and 290 cm^{-1} signals, each marked as lines.

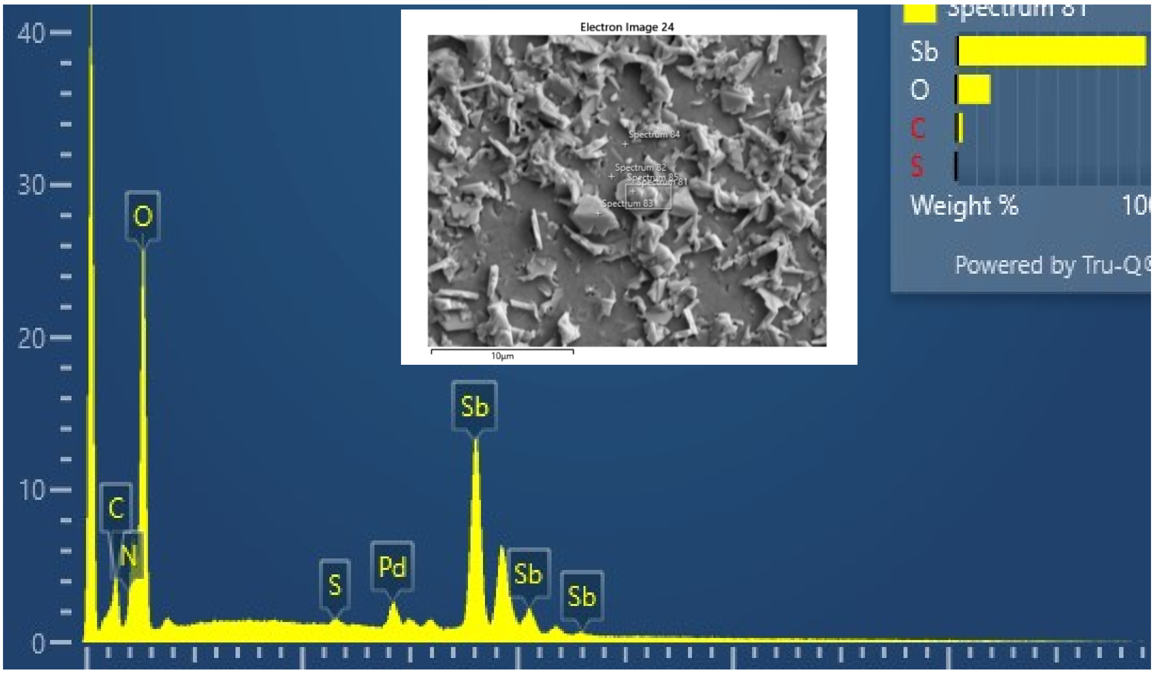

Supplementary Figure 4: SEM-EDS of surface particles on standard Sb_2S_3 film with corresponding SEM image inset.

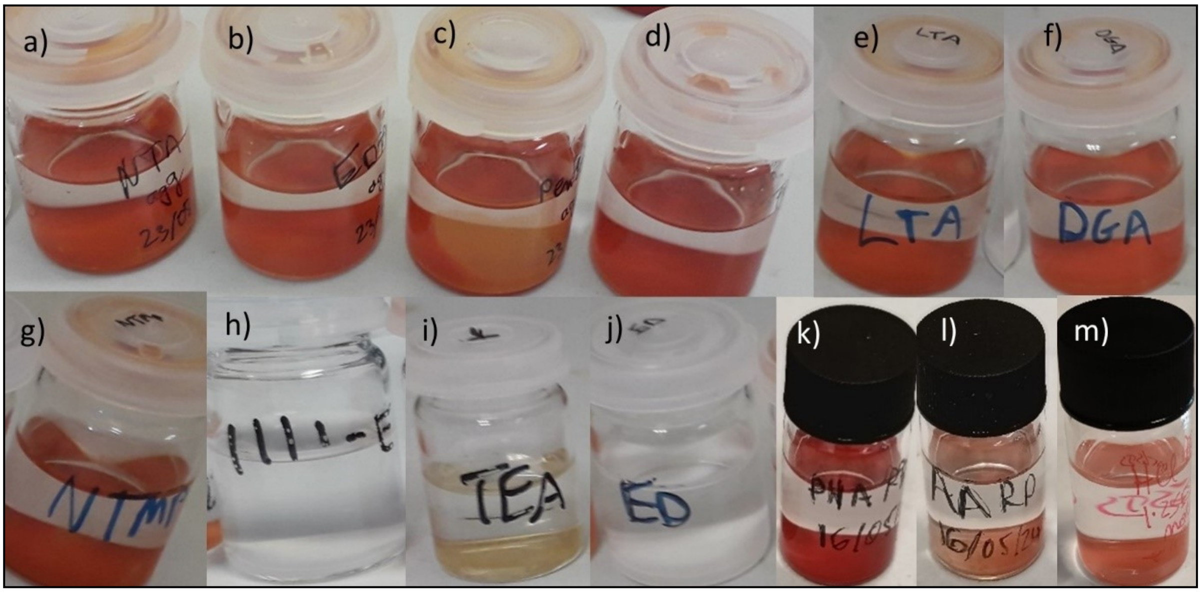

Supplementary Figure 5: Result of screening process for additives a) EDTA, b) NTA, c) PA, d) TETAH, e) LTA, f) DGA, g) NTMP, h) 1111E, i) TEA, j) ED, k) PHA, l) AA, and m) HCl.

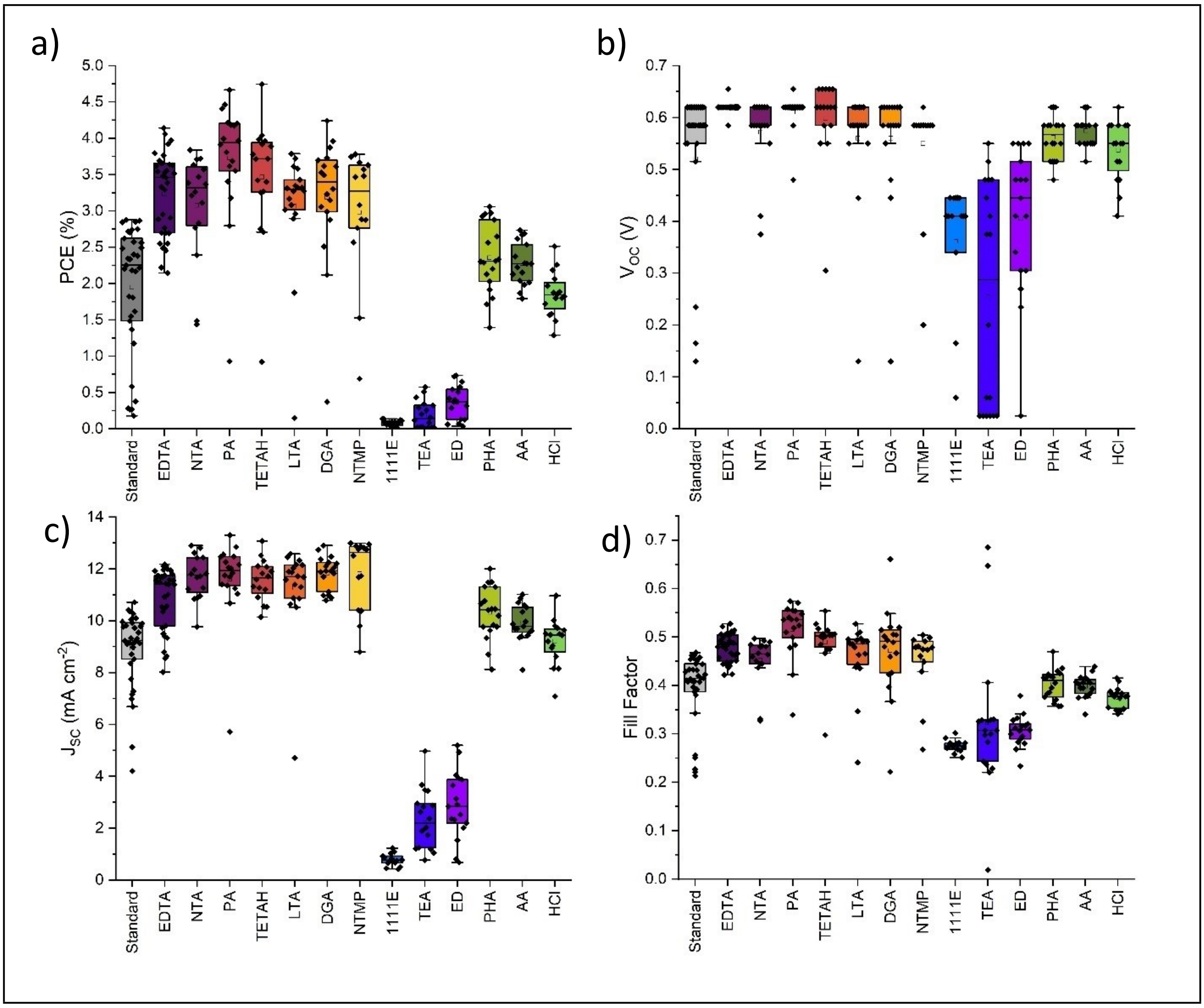

Supplementary Figure 6: Statistics for cell performance characteristics a) PCE, b) V_{OC}, c) J_{SC} and d) FF of Sb_2S_3 solar cells made using additives from Table 1. 6 cells were tested for standard and EDTA, and 3 were tested for each other additive. Each cell had 6 pixels, giving a total of 36 pixels for standard and EDTA, and 18 for the other additives. Shunted pixels did not yield photovoltaic performance and so were excluded. In total, one pixel of the standard, EDTA, AA and ED, two pixels of the NTA, TETAH and HCl, three of the 1111E and four of the NTMP pixels were fully shunted and thus excluded from the results.

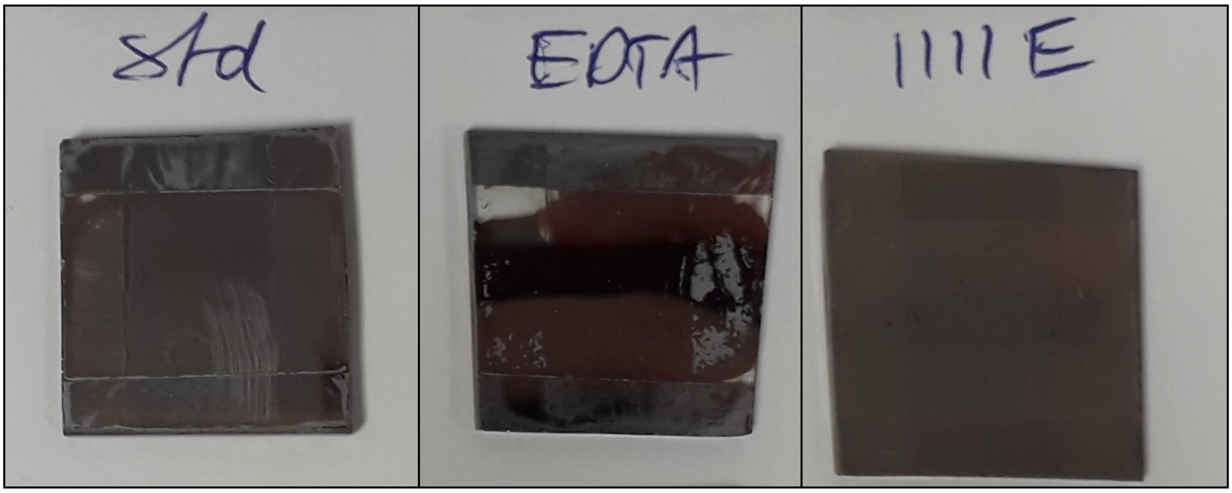

Supplementary Figure 7: Examples of Sb_2S_3 films formed using (from left to right) no additive (standard), EDTA, and 1111E. EDTA (a red powder forming additive) makes the film appear shiny and mirror-like, while 1111E (a white powder forming additive) creates a very rough surface with little to no shine. The standard has properties in between the two.

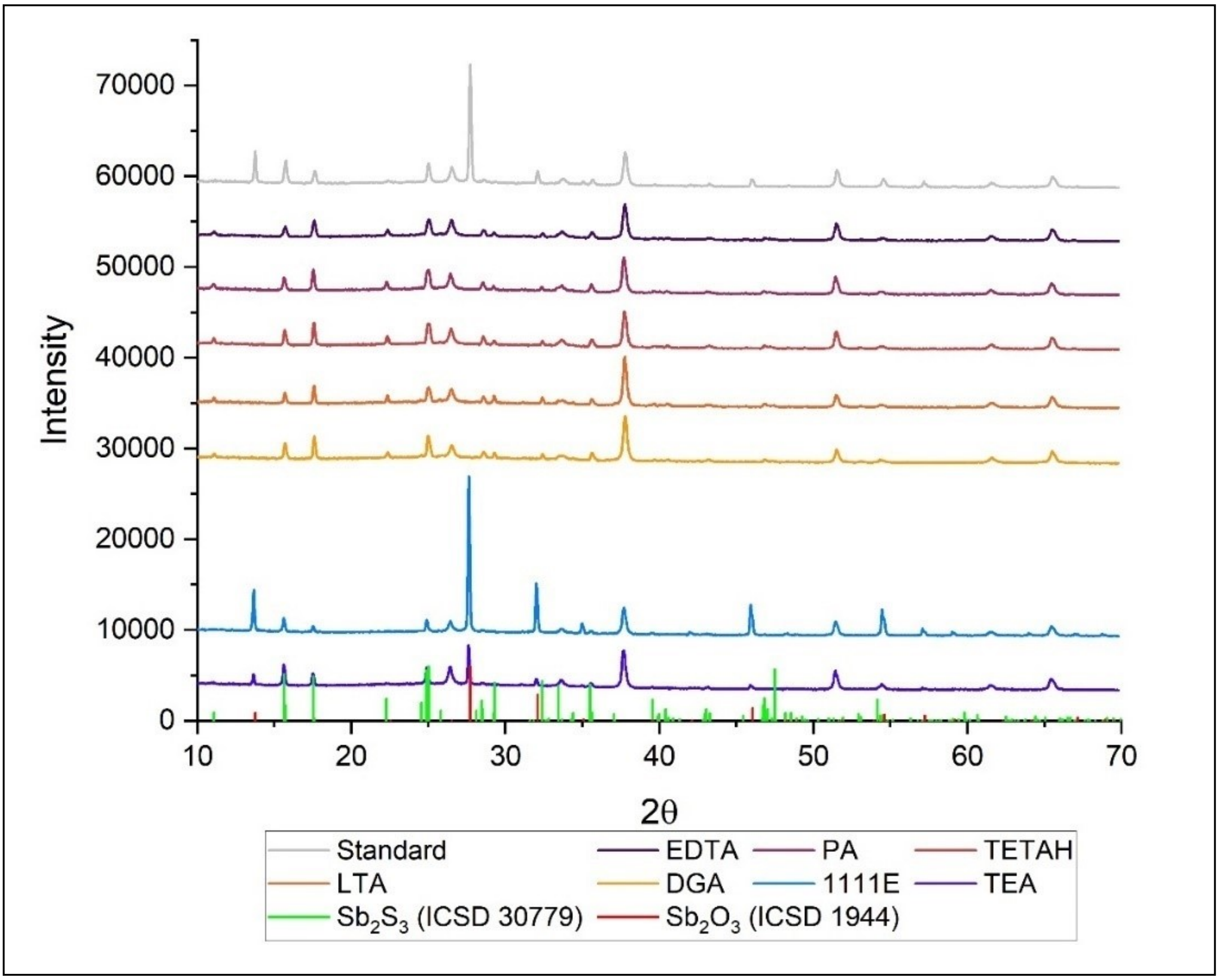

Supplementary Figure 8: Powder XRD of Sb_2S_3 films made using a selection of additives from Table 1, alongside ICSD standards for Sb_2S_3 (collection code 30779) and Sb_2O_3 (collection code 1944).

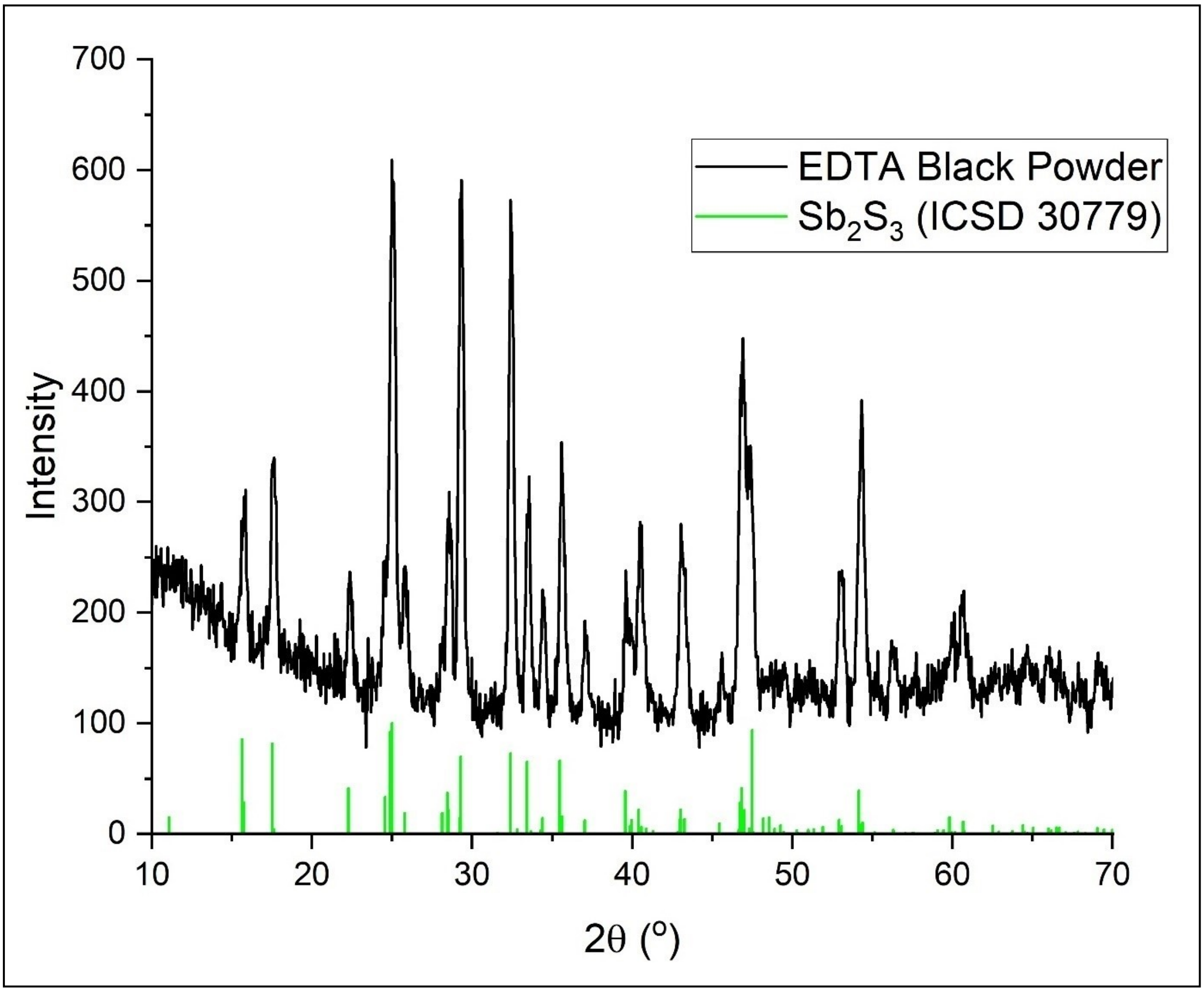

Supplementary Figure 9: Powder XRD of black powder formed by annealing red precipitate of EDTA aggregation test at 350 °C for 10 minutes under N_2, with reference Sb_2S_3 peaks (ICSD collection code 30779).

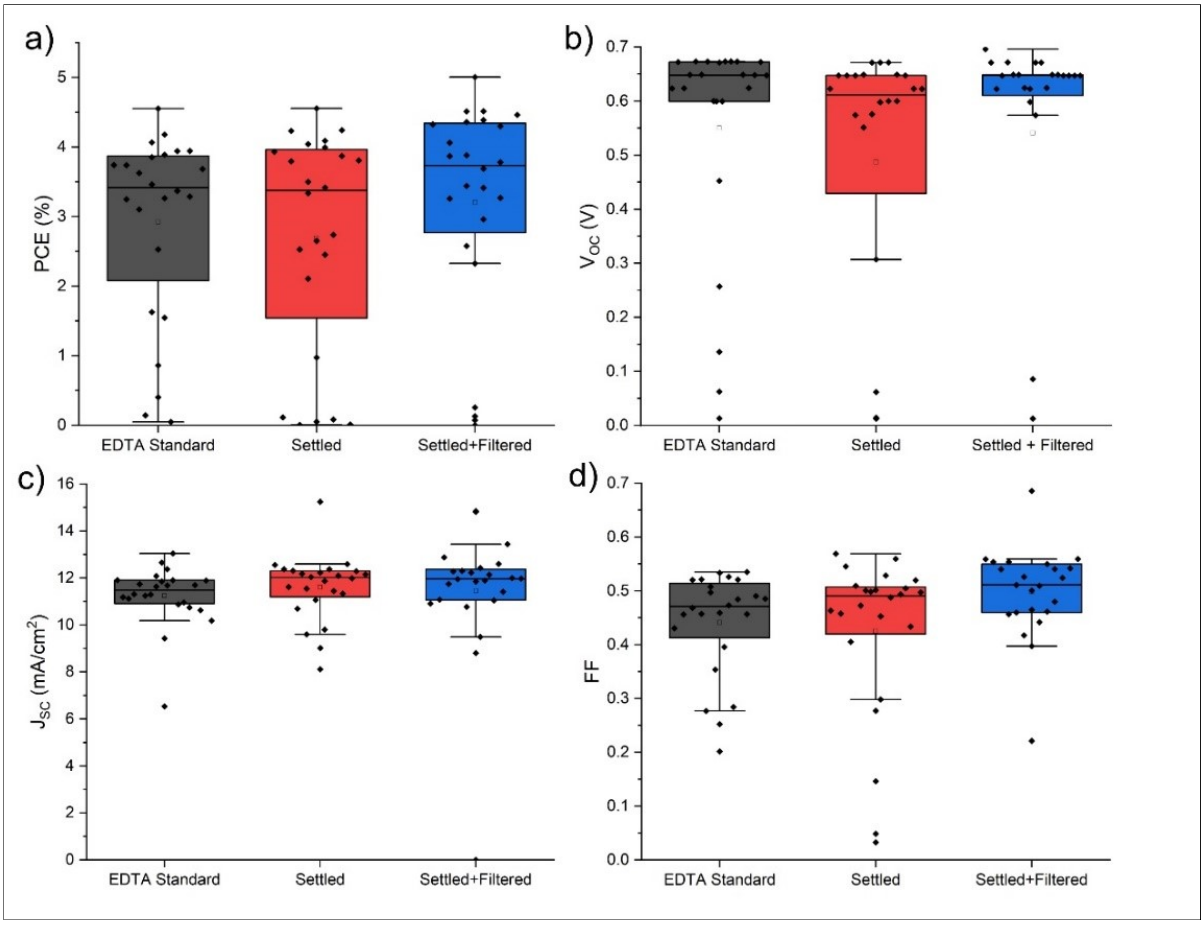

Supplementary Figure 10: Statistics for cell performance characteristics a) PCE, b) V_{OC}, c) J_{SC} and d) FF of Sb_2S_3 solar cells made using i) EDTA with no change (EDTA Standard), ii) allowing the red powder to form in the hydrothermal solution over a day (Settled), and iii) allowing the red powder to form, then filtering it out (Filtered). A total of 4 cells were made for each condition. Each cell had 6 pixels, totalling 24 pixels per condition.

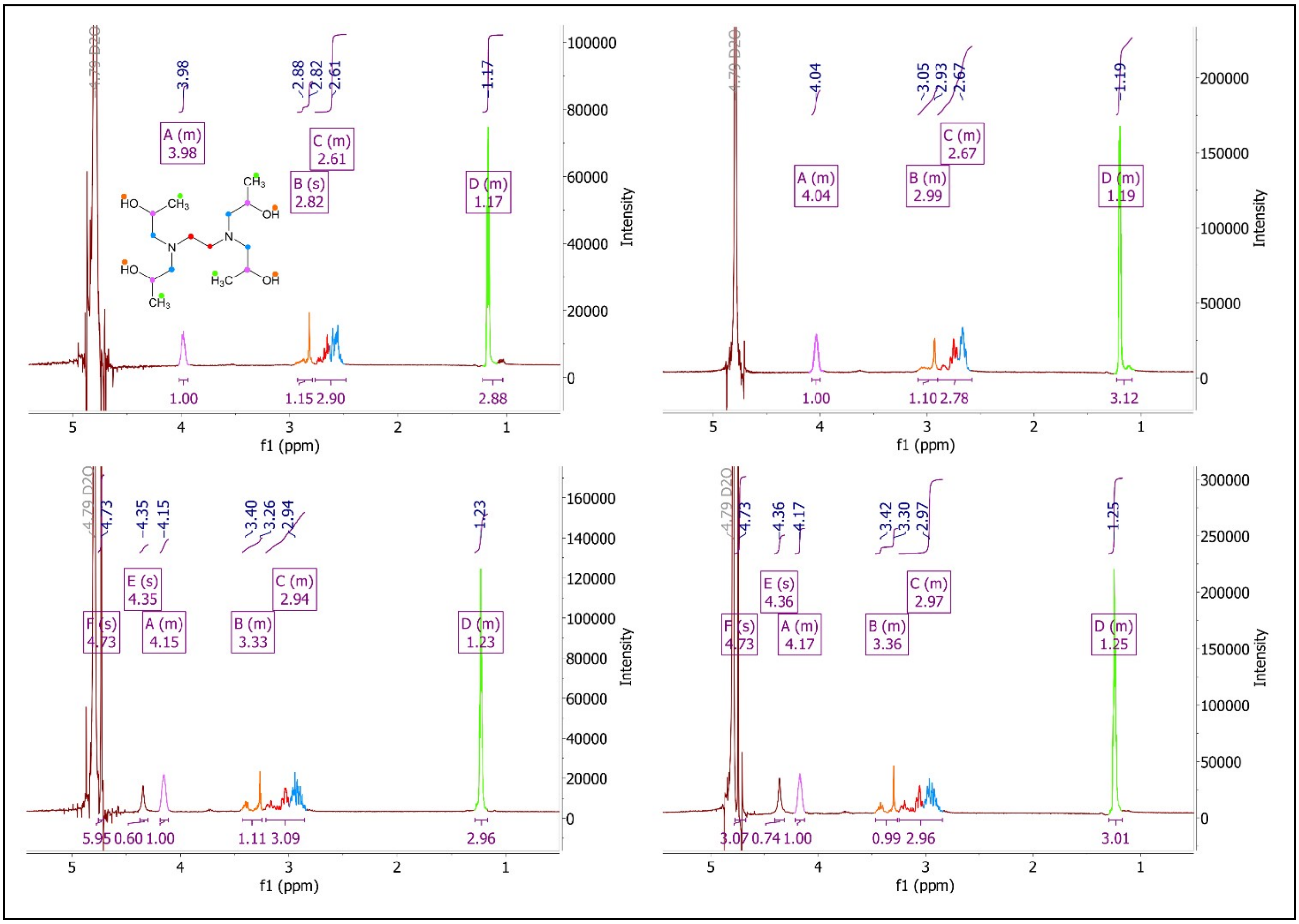

Supplementary Figure 11: ^{1}H NMR spectra of solution containing a) 1111E in D_2O, showing relative assignments of peaks to groups in 1111E structure, b) 1111E + STS in D_2O, c) 1111E + PAT in D_2O and d) 1111E + STS + PAT in D_2O.

Supplementary Table 1: SEM-EDS results of annealed and unannealed standard, EDTA and PA films, and annealed and unannealed EDTA and PA screening test powders. Values are a weight percentage of that element in the tested sample, averaged over at least 4 measurements in different locations.

Sample	C (wt%)	N (wt%)	O (wt%)	Na (wt%)	K (wt%)	S (wt%)	Ti (wt%)	Sn (wt%)	Sb (wt%)
Standard film (unannealed)	2.69	0.21	9.35	0	0	11.16	3.76	32.09	40.76
Standard film (annealed)	3.06	0.53	11.40	0	0	10.88	3.36	32.00	38.76
EDTA film (unannealed)	3.39	0.15	5.80	0	0	16.93	2.57	21.05	50.11
EDTA film (annealed)	3.08	0.93	5.99	0	0	16.39	2.65	22.60	48.35
EDTA red powder (unannealed)	3.74	0.24	2.76	0.17	0	24.05	0	0	69.03
EDTA red powder (annealed)	0	0	4.06	1.03	0.39	24.66	0	0	69.86
PA film (unannealed)	14.10	0	4.80	0	0	16.15	1.93	15.42	47.60
PA film (annealed)	15.04	0	3.68	0	0	17.27	1.60	11.94	50.48
PA red powder (unannealed)	10.13	0	4.08	0.32	0	20.51	0	0	64.97
PA powder (annealed)	9.07	0	4.49	0.30	0	19.32	0	0	66.82

Supplementary Table 2: Champion and average cell performance characteristics of PCE, V_{OC}, J_{SC} and FF with standard deviations for standard cell and cells made with each additive listed in Table 1.

Additive	**PCE (%) champion, (average ±s.d.)**	**V_{OC} (V) champion, (average ±s.d.)**	**J_{SC} (mA cm^{-2}) champion, (average ±s.d.)**	**FF champion, (average ±s.d.)**
Standard (none)	2.88 (1.95 ±0.86)	0.62 (0.52 ±0.17)	10.05 (8.94 ±1.45)	0.46 (0.39 ±0.08)
EDTA	4.14 (3.23 ±0.56)	0.66 (0.62 ±0.02)	12.12 (10.87 ±1.18)	0.52 (0.48 ±0.03)
NTA	3.84 (3.08 ±0.72)	0.62 (0.57 ±0.07)	12.90 (11.69 ±0.82)	0.48 (0.45 ±0.05)
PA	4.67 (3.73 ±0.82)	0.66 (0.61 ±0.04)	13.30 (11.60 ±1.57)	0.54 (0.52 ±0.06)
TETAH	4.75 (3.47 ±0.82)	0.66 (0.60 ±0.08)	13.07 (11.57 ±0.76)	0.55 (0.49 ±0.05)
LTA	3.79 (3.06 ±0.82)	0.62 (0.56 ±0.11)	12.45 (11.26 ±1.70)	0.49 (0.46 ±0.07)
DGA	4.24 (3.19 ±0.85)	0.62 (0.56 ±0.11)	12.47 (11.84 ±0.63)	0.55 (0.47 ±0.09)
NTMP	3.78 (2.98 ±0.87)	0.59 (0.55 ±0.11)	12.81 (11.81 ±1.35)	0.50 (0.45 ±0.07)
1111E	0.14 (0.08 ±0.04)	0.41 (0.25 ±0.21)	1.23 (2.35 ±1.08)	0.27 (0.28 ±0.14)
TEA	0.57 (0.19 ±0.18)	0.48 (0.36 ±0.12)	3.67 (0.78 ±0.22)	0.33 (0.32 ±0.01)
ED	0.74 (0.37 ±0.22)	0.55 (0.41 ±0.14)	3.92 (2.88 ±1.25)	0.34 (0.31 ±0.03)
PHA	3.06 (2.36 ±0.47)	0.59 (0.56 ±0.04)	12.00 (10.32 ±0.99)	0.44 (0.40 ±0.03)
AA	2.73 (2.27 ±0.28)	0.62 (0.57 ±0.03)	10.87 (9.91 ±0.69)	0.41 (0.40 ±0.02)
HCl	2.51 (1.85 ±0.30)	0.59 (0.54 ±0.06)	10.97 (9.20 ±0.87)	0.39 (0.37 ±0.02)

Supplementary References

1. L. Zhang, W. Lian, X. Zhao, Y. Yin, T. Chen and C. Zhu, *ACS Applied Energy Materials*, 2020, **3**, 12417-12422.
2. S. Barthwal, R. Kumar and S. Pathak, *ACS Applied Energy Materials*, 2022, **5**, 6545-6585.
3. Y. Zeng, J. Huang, J. Li, K. Sun, U. A. Shah, H. Deng, X. Zhang, C. Sha, C. Qian, H. Song and X. Hao, *Solar RRL*, 2022, **6**, 2200435.
4. L. Wang, D.-B. Li, K. Li, C. Chen, H.-X. Deng, L. Gao, Y. Zhao, F. Jiang, L. Li, F. Huang, Y. He, H. Song, G. Niu and J. Tang, *Nature Energy*, 2017, **2**, 17046.
5. P. K. Nair, M. T. S. Nair, V. M. Garcı́a, O. L. Arenas, A. C. Y. Peña, I. T. Ayala, O. Gomezdaza, A. Sánchez, J. Campos, H. Hu, R. Suárez and M. E. Rincón, *Solar Energy Materials and Solar Cells*, 1998, **52**, 313-344.
6. R. Parize, A. Katerski, I. Gromyko, L. Rapenne, H. Roussel, E. Kärber, E. Appert, M. Krunks and V. Consonni, *The Journal of Physical Chemistry C*, 2017, **121**, 9672-9680.